

Article

**Off-Lattice Simulation of Multifunctional Monomer
Polymerizations: Effects of Monomer Mobility, Structure,
and Functionality on Structural Evolution at Low Conversion**

J. Brian Hutchison, and Kristi S. Anseth

J. Phys. Chem. B, **2004**, 108 (30), 11097-11104 • DOI: 10.1021/jp049390s • Publication Date (Web): 25 June 2004

Downloaded from <http://pubs.acs.org> on April 9, 2009

More About This Article

Additional resources and features associated with this article are available within the HTML version:

- Supporting Information
- Links to the 1 articles that cite this article, as of the time of this article download
- Access to high resolution figures
- Links to articles and content related to this article
- Copyright permission to reproduce figures and/or text from this article

[View the Full Text HTML](#)



Off-Lattice Simulation of Multifunctional Monomer Polymerizations: Effects of Monomer Mobility, Structure, and Functionality on Structural Evolution at Low Conversion

J. Brian Hutchison[†] and Kristi S. Anseth^{*,†,‡}

Department of Chemical and Biological Engineering, and Howard Hughes Medical Institute, University of Colorado, Boulder, Colorado 80309-0424

Received: February 10, 2004; In Final Form: May 12, 2004

Fundamental insight into the polymerization behavior and structural evolution of highly cross-linked polymers synthesized from the chain polymerization of multifunctional monomers will benefit a number of current and emerging applications. This contribution reintroduces¹ an off-lattice kinetic gelation model with refinements to the representations of monomer mobility, structure, and functionality, which more realistically capture low conversion propagation events during cross-linked network evolution. Intramolecularly cross-linked macromolecules (ICMs) are formed by simulation of a single propagating radical within a volume containing ca. 100 000 monomer units. Effects of monomer mobility, structure, and functionality on the relative size, kinetic chain length, and intramolecular cross-link density of ICMs are reported. Finally, aspects of percolation theory are applied to this off-lattice kinetic gelation simulation. The fractal dimension corresponds to the theoretical value for a lattice animal created by a three-dimensional percolation model and it is independent of conversion. Overall, this contribution demonstrates the utility of a unique approach for kinetic gelation simulation of multifunctional monomer polymerizations that affords more realistic representation of monomer structure and dynamics than traditional, lattice-based models.

Introduction

Physical and mechanical properties of highly cross-linked polymeric networks include, among others, insolubility and high mechanical strength, which are desirable for a number of commercial and emerging applications. In particular, highly cross-linked polymers synthesized by the photoinitiated chain polymerization of multifunctional monomers are used for coatings,^{2,3} flexographic printing plates,⁴ and dental restorative materials.⁵ A unique and beneficial aspect of this materials processing method is that the liquid reactants form a solid product that is fabricated directly into its useful form. Because of the inability to further process cross-linked networks, traditional applications, along with emerging areas in biomaterials,^{6,7} tissue engineering scaffolds,^{7–9} and microfabrication,^{10–13} require fundamental knowledge and understanding of the evolution of cross-linked macromolecular structure during the polymerization of multifunctional monomers to control the final material properties.

Over the past several decades, many authors have contributed to the current, qualitative model of structural evolution from multifunctional monomer polymerizations that accounts for various aspects of polymerization kinetics, as well as indirect inferences and direct observations of film inhomogeneities.^{2,14–19} Specifically, distinct regions of highly cyclized and cross-linked polymer form prior to macroscopic gelation. The regions of polymer become more highly cross-linked due to (1) enhancement of pendant double bond concentration in the vicinity of the propagating macroradical (relative to monomeric vinyl groups) and (2) minimization of bimolecular termination due to macroradical diffusion limitations, which results in higher

bulk and local radical concentrations. In fact, the restricted diffusion of macroradicals leads to significant radical trapping within highly cross-linked networks formed from multifunctional monomer polymerizations.^{20,21} At the point of macroscopic gelation, local regions of polymer—microgels—react with each other via pendant unsaturation at their peripheries. Finally, despite the presence of unreacted double bonds and continued initiation, significant residual unsaturation, trapped radicals, and nanoscale heterogeneity remain.

Since experimental characterization of multifunctional monomer polymerizations and the resulting insoluble networks is difficult, simulations of network formation provide an avenue to acquire fundamental knowledge and test hypotheses related to experimental observations. Three methods for modeling polymerizations of multifunctional monomers prevail: statistical, kinetic, and kinetic gelation approaches.^{22,23} Statistical models, kinetic models, and combinations of the two each yield unique structural information such as gel and sol fractions, molecular weight between cross-links, the number of elastically active chains, and polymerization rate behavior. However, usually these models are based on mean-field averages of rate parameters and concentrations, so heterogeneity is not captured and/or included in many cases.

The third approach is simulation of structural evolution in space—percolation or kinetic gelation models—that provides information about structure in local regions during gelation. This type of simulation is useful for multifunctional monomer polymerizations that are characterized by gelation at low conversion since individual species are fixed on a regular lattice array within the simulation box from the onset (i.e., mobility is restricted). The advantage of this type of simulation is the elimination of mean-field averages and the ability to capture polymerization heterogeneities and behavior during network formation. Conversely, designation of monomer units as fixed

* Address correspondence to this author.

[†] Department of Chemical and Biological Engineering.

[‡] Howard Hughes Medical Institute.

lattice points results in unrealistic representation of species dynamics and immobility at low conversion. Thus, simulations that afford greater detail related to monomer structure, energetics, and mobility would provide a significant advance and contribution to fundamental insight regarding structural evolution during the polymerization of multifunctional monomers.

Background

The basic premise of the kinetic gelation approach is intuitive. In general, a specific number of monomers with reactive ends are positioned at fixed points in a reaction volume. A specified fraction of reactive ends is “seeded” with active radicals, and these radicals propagate via a random walk through unreacted local ends (i.e., unsaturated bonds). Termination of these active radicals occurs by combination with another radical (i.e., bimolecular termination) or propagation may cease when the local environment of the radical does not contain any unreacted particle ends—radical trapping.

Manneville and de Seze²⁴ developed the first kinetic gelation model, a percolation type model, that was used to investigate critical behavior related to the statistical distribution of bonds between neighboring or second-neighboring monomer units. Evolution of the kinetic gelation modeling approach included characterization of different variations of models in terms of a universality class differing from classical gelation theories or random percolation models and reflecting differences in the underlying mechanism of network formation.^{25–29} Early refinements to the kinetic gelation approach included implementation of various complexities to simulate monomers and polymerization conditions more realistically, utilization of simulations to predict qualitative trends, and comparison of simulation results to experimental data. Specifically, various authors have contributed approaches for the following: increased monomer mobility and incorporation of solvent;^{30–35} improved or different representations of initiation “rate” and initiator structure;^{36–39} specific investigation of macromolecular and network structural heterogeneities (e.g., cyclization, microgelation, and monomer pool formation);^{40–45} and exploration of conversion-dependent behavior at various polymerization conditions.^{2,35,38,41,46–50} However, most of the investigations of multifunctional monomer polymerizations by kinetic gelation approaches suffer from unrealistic simulation of monomer structure and mobility due to the fixed lattice representation of three-dimensional space.

Combining aspects of kinetic gelation, Monte Carlo statistical algorithms and molecular dynamics approaches have begun to address the primary shortcoming of traditional kinetic gelation models—the lattice representation of monomers. For example, combinations of statistical analyses with off-lattice percolation theory have been introduced to explore intramolecular cross-linking and/or cyclization^{51–54} and diffusional effects.⁵⁵ An approach in which monomers react during a molecular dynamics simulation⁵⁶ provides very detailed information about molecular structure of cross-linked monomers at a high computational cost. Finally, an off-lattice kinetic gelation simulation to investigate chain polymerization of liquid crystalline monomer systems^{57,58} was a precursor to a more universal off-lattice kinetic gelation model that simulates polymerization of multifunctional monomers other than liquid crystalline monomers.¹

Simulations combining mobility and particle interactions during polymerization reactions represent a separate class of models that, to this date, has not been fully developed or implemented. In particular, exploration of structural evolution at low conversion (i.e., prior to macroscopic gelation) requires realistic representation of monomers. Furthermore, according

to widely accepted theory, independent initiation events, which create local regions of macromolecular structure, may have a large impact on subsequent structural evolution (i.e., microgel formation) and final network properties.

Simulation Description

This contribution reports modifications to an off-lattice simulation developed previously¹ to impart more realistic propagation events by altering monomer and macroradical structure. In addition, this model is applied to exploration of macromolecular structure evolving from single radicals prior to macroscopic gelation. Specifically, formation of intramolecularly cross-linked macromolecules (ICMs) is simulated, and intramolecular cross-link density, kinetic chain length, and radius of gyration are reported as a result of simulation parameters including monomer mobility, monomer structure as defined by the angle between double bonds on a monomer sphere, and monomer functionality by including 50% monovinyl monomers.

General Simulation Aspects. The off-lattice simulation approach implemented in this contribution has been described in detail elsewhere.¹ Lennard-Jones spheres represent the individual monomer species within a three-dimensional box with periodic boundary conditions. Movements of the monomer units are accepted or rejected based on the Metropolis criteria,⁵⁹ which account for the change in potential energy of the entire simulation volume due to a proposed change in the spatial position of a single monomer unit. Two reactive ends on each monomer molecule are located on the sphere surface. Polymerization of these reactive sites proceeds by specific rules, consistent with a chain propagation mechanism. Information pertaining to several structural features, including the fraction of intramolecular cross-links, propagating radical history (i.e., kinetic chain length), trapped radicals, unreacted monomer, and conversion of double bonds, is compiled.

Specific aspects of the simulation routine include initialization of the box; initiation, propagation, and termination reactions; and species mobility (e.g., diffusion and/or relaxation). Initialization of the box is accomplished by equilibrating a regular array of Lennard-Jones spheres. First, particles are distributed uniformly with a defined overall density. For the results presented in this contribution, the volume of monomers was 50% of the total volume. The ordered box is randomized through the monomer mobility mechanism until the overall radial distribution function changes from that of a regular array to the characteristic liquid form.

From this starting point, simulation parameters were chosen to examine and study the formation of individual intramolecularly cross-linked macromolecules (ICMs). Specifically, after equilibration, one of the particle ends in a simulation volume containing ca. 100 000 monomer units is selected randomly and designated as an active radical. At each reaction step, the closest unreacted particle end to the propagating radical, within a defined “reaction volume”, is found. A bond is created between the active radical site and the unreacted end as the active radical propagates (moves) to the new end. The bond is relaxed to a minimum energy length, and the local region of particles is reequilibrated. Propagation and reequilibration continue until no unsaturated ends are available within the reaction volume of the active radical. This radical trapping mechanism for termination is implemented to capture structural evolution independent of bimolecular termination (i.e., at low radical concentrations).

Individual ICMs form randomly, within constraints of monomer mobility and structure, and radical trapping is determined by highly localized structure (i.e., it is not prede-

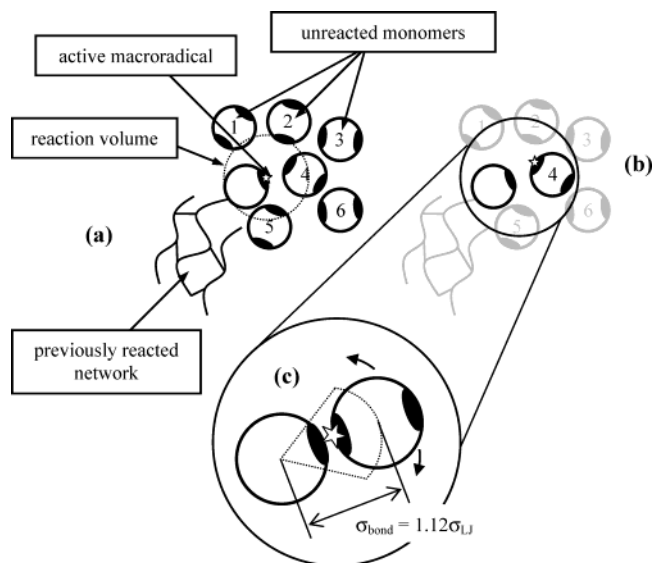


Figure 1. Propagation sequence. (a, b) An active radical, which is located at one end of a divinyl monomer represented by a Lennard-Jones sphere, selects the nearest unreacted end within a predefined reaction volume and propagates to the new end. (c) If the newly reacted end was previously unreacted (i.e., the monomer contains a pendant vinyl group), then the newly reacted monomer translates to the Lennard-Jones minimum energy separation distance and reorients to minimize the local potential energy.

terminated by the overall conversion). Therefore, a number of ICMs were generated for each different set of conditions to estimate the variance in different responses (e.g., kinetic chain length, radius of gyration, etc.) and draw conclusions about the effects of various parameters on these responses. Results are reported as an estimated mean with error bars that indicate 90% confidence intervals. The number of individual ICMs generated to create each point is indicated in each figure.

Monomer Mobility. Each monomer unit, which is represented as a Lennard-Jones sphere, has translational and rotational mobility. Rotational moves do not affect the potential energy calculation since each monomer is a sphere. Thus, rotational moves are always accepted, but translational moves must meet the Metropolis criteria for acceptance. The ratio of translational versus rotational velocity for a liquid monomer was estimated as ca. 100.⁶⁰ Therefore, the frequency and average length of attempted translational steps relative to rotational events were predetermined to yield an appropriate ratio of translational distance (i.e., product of the frequency of accepted moves and the average accepted step length) to rotational distance.

Two parameters dictate the relative reactivity and mobility of monomers and macroradicals in the simulation. First, the number of local equilibration events (i.e., random selection and attempted movements of monomer units that are in the vicinity of the propagating radical) between reaction events represents monomer mobility (i.e., diffusion). Second, the space that a propagating radical searches for unreacted vinyl groups represents a combination of the segmental mobility of the macroradical species and the accessibility of unreacted groups in the local region of an active radical.

Macroradical Growth. Upon selection of the closest unsaturated vinyl group within a specified reaction volume, the active radical is transferred to the new position. If the new group is part of an unreacted monomer (i.e., not pendant functionality), then prior to equilibration of monomer in the local region, the new bond relaxes to a specified length and minimum energy orientation. Figure 1 depicts the process of bond selection and

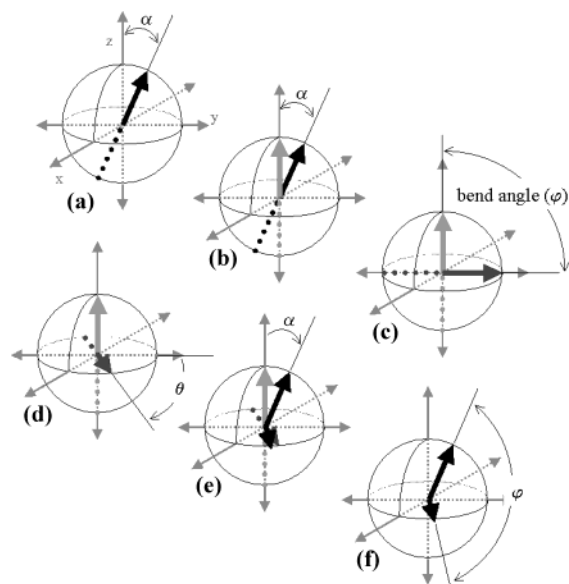


Figure 2. Random orientation of a defined divinyl bond angle. (a, b) The orientation of one vinyl group (α) is measured relative to the z -axis and the monomer sphere is reoriented along that axis. (c) The second vinyl group is positioned at a predefined angle φ (between 0 and 180°) in the y - z plane. (d) The monomer sphere is rotated through a random angle θ (between 0 and 360°) in the x - y plane. (e, f) The sphere is reoriented by the angle α , measured in the first step (a).

positioning. First, the nearest unreacted vinyl group (i.e., from monomer 4) is selected from the unreacted groups located within a predefined volume centered around the macroradical (Figure 1a,b). Then, the radical (depicted as a star) is transferred (i.e., propagates) to the new position. As shown in Figure 1c, the newly reacted monomer is repositioned so that the reacted vinyl group orientation is in line with the newly formed bond. The distance between the newly reacted monomer sphere and the sphere from which the radical was moved is set to the Lennard-Jones minimum energy displacement (i.e., ca. 1.12 σ_{LJ}). Finally, while maintaining the predefined bond length, the orientation of the new bond is adjusted 1000 times to minimize the local potential energy.

Monomer Structure and Functionality. Each monomer unit contains two vinyl groups positioned on the periphery of a Lennard-Jones sphere. Previously,¹ vinyl groups were positioned 180° apart. However, a more realistic representation of monomer molecules may require variable bond orientation. Figure 2 describes the method for positioning two bonds at a fixed angle on a sphere with a completely random orientation. Figure 2a,b shows measurement of the orientation (α) of the first vinyl group relative to the z -axis in a normal Cartesian coordinate system. Figure 2c shows generation of a second vinyl group at a predefined angle φ (between 0 and 180°) in the y - z plane. Figure 2d shows rotation through a random angle θ (between 0 and 360°) in the x - y plane. Finally, Figure 2e,f shows repositioning of the sphere by the angle α , measured in the first step (i.e., Figure 2a). This procedure yields random positions of two vinyl groups, with a fixed angle between them, on the surface of a monomer sphere. In fact, this procedure is also useful for positioning vinyl groups with a unique *distribution* of separation angles to represent a monomer with well-known structure. The facile designation of monomer structure, although relatively simple in this case, provides a significant improvement in the molecular level detail captured by the off-lattice kinetic simulation.

The number of vinyl groups per monomer (i.e., monomer functionality) is another simulation parameter that can be varied

to afford realistic representation of multifunctional monomer copolymerizations. To simulate a comonomer formulation containing 50% monovinyl units, half of the divinyl monomers were selected and one vinyl group on each monomer was designated as unreactive.

Radius of Gyration Calculation. The size of ICMs must be quantified to evaluate trends due to changes in simulation parameters. The equation for calculating the radius of gyration (R_G) for a random coil (i.e., the root-mean-square distance of individual monomers from the center of mass of the ICM) is reported in eq 1.⁶⁰

$$R_G = \left(\frac{\sum r_i^2}{N} \right)^{1/2} \quad (1)$$

Calculation of R_G requires two pieces of information: the distance (r_i) of each individual monomer reacted into the ICM from the ICM center of mass, and the number of monomers incorporated into the ICM (N). Determination of the ICM center of mass requires minimizing the average distance between all reacted monomers and an arbitrary point. In fact, the center of mass does not need to be determined independent of the radius of gyration; radii of gyration are calculated for a set of evenly spaced points distributed regularly throughout the simulation volume. The point corresponding to the minimum R_G is the center of mass, and R_G is known. In the case of the simulation presented here, trial points were spaced at ca. $0.5\sigma_{LJ}$, so the center of mass is found with uncertainty less than $0.5\sigma_{LJ}$.

Results and Discussion

Qualitative Descriptions of Simulated ICMs. A valuable aspect of the off-lattice kinetic gelation simulation is the generation of visual images of individual macromolecules and cross-linked networks formed from multifunctional monomer polymerizations. Figure 3 contains sequential images of an ICM formed from a single radical in a simulation volume containing ca. 100 000 divinyl monomer spheres. Singly reacted monomers are light gray, doubly reacted monomers are dark gray, and unreacted monomers are not shown. Images a–c in Figure 3 show that an elongated structure evolves with doubly reacted monomers clearly dispersed with singly reacted monomers. The step from image c to image d depicts reaction of only 10 vinyl groups, but it reveals the effect of periodic boundary conditions. A radical propagates through the periodic boundary (right face) of the simulation volume to a monomer located at the opposite side (left face). In fact, images d and e in Figure 3 show that the propagating radical travels back and forth through the periodic boundary at least once more. The final ICM structure is shown in Figure 3e. Here 720 vinyl groups are reacted and 508 monomers are incorporated within the ICM prior to trapping of the propagating radical.

Quantitative Comparison of Simulated ICM Characteristics. In addition to qualitative images of ICMs, quantitative comparisons of a number of characteristics can be made in response to changes in parameters that dictate relative reactivity, mobility, monomer structure, and so forth. In particular, Figure 4 contains plots of different ICM characteristics, measured after radical trapping, as a function of the qualitative level of monomer mobility. In this case, two vinyl groups on each monomer sphere were randomly oriented with a 60° angle between them, and the radius that defined the “reaction volume” was set at $1.0\sigma_{LJ}$. Figure 4a shows the effect of monomer mobility on the number of vinyl groups reacted by a single radical—the kinetic chain length. Since radical trapping de-

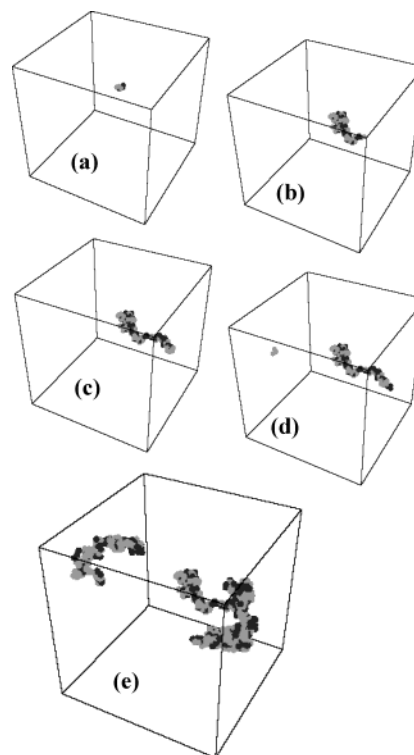


Figure 3. Qualitative images of a simulated ICM. Each cube represents the simulation volume that contains 97 336 monomers. Singly reacted monomers are light gray, doubly reacted monomers are dark gray, and unreacted monomers are not shown. (a–c) An elongated structure evolves with doubly reacted monomers dispersed with singly reacted monomers. (c, d) The effect of periodic boundary conditions is revealed; a radical propagates through the periodic boundary (right face) of the simulation volume to a monomer located at the opposite side (left face). (e) 720 vinyl groups are reacted and 508 monomers are incorporated within the ICM prior to trapping of the propagating radical.

creases with increasing mobility,¹ more vinyl groups are reacted when mobility is increased. Figure 4b shows the radii of gyration, normalized by σ_{LJ} , for three levels of monomer mobility. Similar to the kinetic chain lengths reported in Figure 4a, radii of gyration increase with increasing mobility. Finally, Figure 4c provides the fraction of doubly reacted monomers (relative to the total number of reacted monomers) as a function of monomer mobility. Interestingly, monomer mobility does not have a significant effect on the fraction of doubly reacted monomers. Upon closer examination, the inset expansion in Figure 4c shows a slight increase in the fraction doubly reacted, albeit with very low statistical significance. On the basis of first principles, an increase in monomer mobility should lead to a higher effective reactivity of monomeric vinyl groups relative to pendant vinyls, which is not in agreement with the results shown in Figure 4c. Two other features of the figure require further examination as well. First, the simulated fraction of doubly reacted monomers is very high: the double bond conversion within the ICMs is greater than 90%. Second, the variance in the fraction of doubly reacted monomers is much lower than the variances found for size measurements (i.e., radius of gyration and kinetic chain length).

A parameter that likely impacts the fraction of doubly reacted monomers is the angle between vinyl groups, because the angle dictates the distance between a propagating site and the pendant group on the same monomer. A smaller angle causes a higher probability for cyclopolymerization (i.e., divinyl loop formation, which is consecutive reaction of double bonds from the same molecule during propagation of a free radical). Figure 5 contains

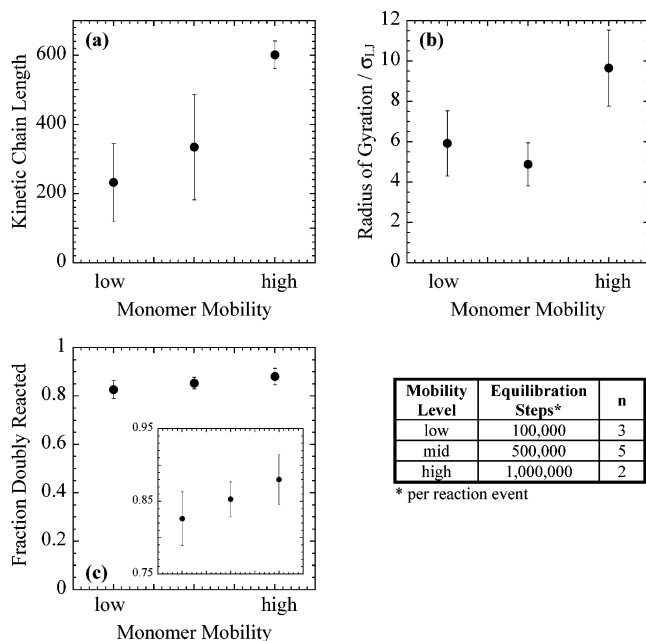


Figure 4. Simulated ICM characteristics relative to monomer mobility. (a) Kinetic chain length (i.e., number of vinyl groups reacted by a propagating radical), (b) radius of gyration (normalized by σ_{LJ}), and (c) the fraction of reacted monomers that are doubly reacted are plotted relative to a qualitative monomer mobility scale. ICM characteristics were measured after trapping of a single radical within a simulation volume containing 97 336 divinyl monomers (divinyl angle, 60° ; reaction volume radius, $1.0\sigma_{LJ}$). Error bars indicate 90% confidence intervals based on the number (n) and standard deviation of responses from repeated simulations of each monomer mobility level.

plots of three ICM characteristics, measured after radical trapping, as a function of the angle between vinyl groups. In this case, the radius that defined the “reaction volume” was set at $1.0\sigma_{LJ}$, and the monomer mobility was fixed at the middle level reported in Figure 4. Figure 5a reveals a large increase in the average kinetic chain length for ICMs formed from monomers with 120° divinyl angles relative to the ICMs made from 60° or 180° monomers. Figure 5b shows a significant increase in the radii of gyration, normalized by σ_{LJ} , for polymerization of monomers with divinyl angles of 60° , 120° , and 180° .

Closer analysis of the fraction of doubly reacted monomers, which is shown in Figure 5c, provides insight into the anomalous behavior displayed in Figure 5a as well as the apparent inconsistency between parts a and b in Figure 5. Solid circles show that the fraction of doubly reacted monomers decreases significantly as a function of divinyl angle. The solid diamonds represent the fraction of reacted monomer units that are divinyl loops. In fact, over 80% of the doubly reacted monomers in ICMs formed from 60° monomers are divinyl loops. The solid squares represent the fraction of doubly reacted monomers that are *not* divinyl loops—intramolecular cross-links. Interestingly, the fractions of intramolecular cross-links are similar for each of the monomer structures.

The results shown in Figures 4 and 5 reveal that the vinyl bond angle plays a critical role in the simulation of ICMs. When the angle is small (e.g., 60°), cyclopolymerization is prevalent and the propagating radical remains within a smaller region of monomers. Eventually, the radical becomes trapped due to reaction of all the accessible vinyl groups within that region. Conversely, when the angle is large (e.g., 180°), divinyl loop formation is minimized, so the ICM grows in a highly extended configuration. Although the overall structure is more extended,

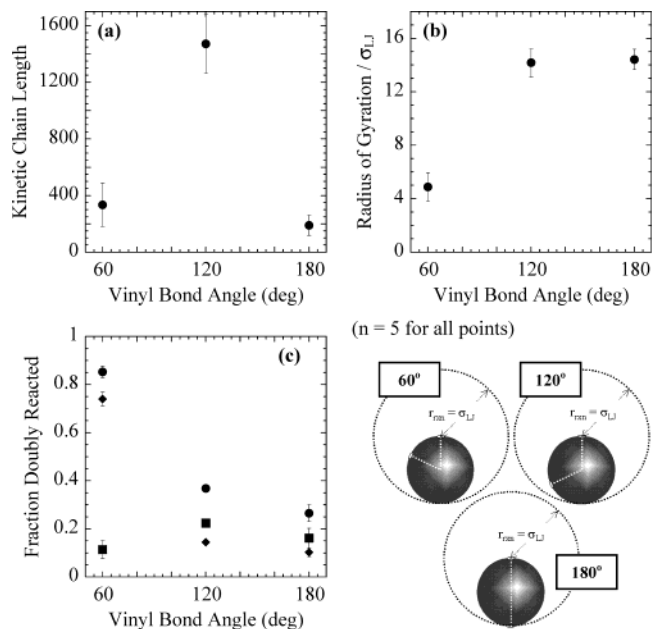


Figure 5. Simulated ICM characteristics relative to divinyl bond angle. (a) Kinetic chain length (i.e., number of vinyl groups reacted by a propagating radical), (b) radius of gyration (normalized by σ_{LJ}), and (c) the fraction of reacted monomers that are doubly reacted (circles), divinyl loops (diamonds), and intramolecular cross-links (i.e., total doubly reacted less divinyl loops; squares) are plotted relative to the angle separating two vinyl bonds that are randomly oriented on each monomer sphere. ICM characteristics were measured after trapping of a single radical within a simulation volume containing 97 336 divinyl monomers (monomer mobility, middle level from Figure 4; reaction volume radius, $1.0\sigma_{LJ}$). Error bars indicate 90% confidence intervals based on the number (n) and standard deviation of responses from repeated simulations with each divinyl angle.

the local concentration of unsaturated groups in the vicinity of the propagating radical is lower, so the average terminal kinetic chain length is short. Finally, for an intermediate divinyl angle (e.g., 120°), the ICM forms in an extended configuration, but accessibility of pendant vinyls provides a route for the radical to escape regions of low unsaturation density. Therefore, ICMs formed from 120° monomers are larger and/or contain more monomers than ICMs formed from 60° or 180° monomers. More importantly, this simple geometric approach represents an additional level of complexity in the simulated description of monomers that will enable testing of hypotheses regarding monomer structure.

Figure 6 shows results from a simulated polymerization of 50% monovinyl and 50% divinyl monomers. The vinyl groups on each divinyl monomer sphere were randomly oriented with a 120° angle between them, and the radius that defined the “reaction volume” was either $1.0\sigma_{LJ}$ (closed circles) or $1.1\sigma_{LJ}$ (open squares). In fact, expansion of the reaction volume results in larger ICMs, as reported in Figure 6a,b. Additionally, these figures show that the kinetic chain lengths and the average radii of gyration for ICMs formed with 50% monovinyl monomers are significantly smaller than their counterparts for ICMs formed from divinyl monomers only. The explanation for this observation is intuitive and consistent with discussion of the results in Figures 4 and 5; increasing the number of potential reaction sites for a propagating radical (by monomer diffusion to the radical or expansion of the volume sampled by the radical) leads to an increase in ICM size before trapping occurs.

Figure 6c is a plot of the fraction of doubly reacted monomers relative to *all* reacted monomers (i.e., including monovinyl units). Comparison of the open square and the closed circle at

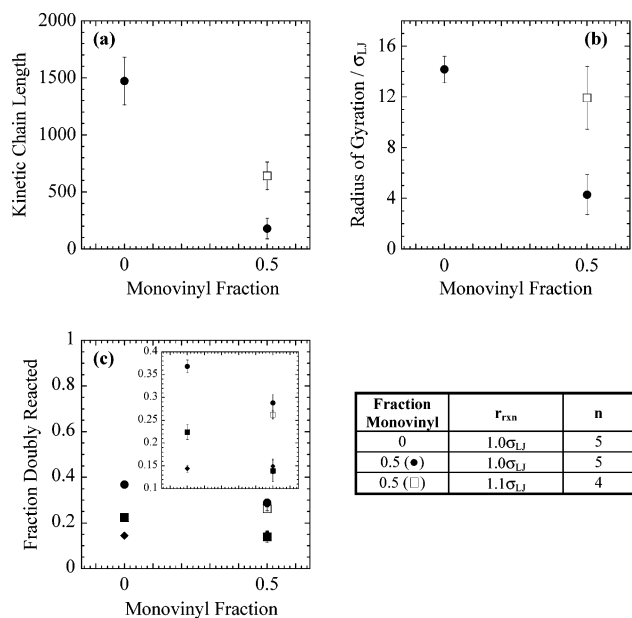


Figure 6. Simulated ICM characteristics relative to monomer functionality. (a) Kinetic chain length (i.e., number of vinyl groups reacted by a propagating radical), (b) radius of gyration (normalized by σ_{LJ}), and (c) the fraction of reacted monomers that are doubly reacted (divinyl loops (diamonds), and intramolecular cross-links (i.e., total doubly reacted less divinyl loops; squares) are plotted relative to the fraction of monovinyl monomers in the simulated monomer formulation. ICM characteristics were measured after trapping of a single radical within a simulation volume containing 97 336 monomers (divinyl angle, 120° ; monomer mobility, middle level from Figure 4). The reaction volume radius was $1.1\sigma_{\text{LJ}}$ for the point on each plot represented by an open square, and it was $1.0\sigma_{\text{LJ}}$ for all other data (solid points). Error bars indicate 90% confidence intervals based on the number (n) and standard deviation of responses from repeated simulations of each monomer functionality level.

the monovinyl fraction of 0.5 indicates that a 10% increase in the radius of the reaction volume does not affect the fraction of doubly reacted monomers. The propagation events that occur between $1.0\sigma_{\text{LJ}}$ and $1.1\sigma_{\text{LJ}}$ facilitate larger terminal ICMs (as shown in Figure 6a,b), but the overall fraction of doubly reacted monomers is not impacted due to the increased reaction volume. Either the propagation events that occur between $1.0\sigma_{\text{LJ}}$ and $1.1\sigma_{\text{LJ}}$ are too few to affect the overall fraction doubly reacted or, more likely, the ratio of radical propagation to unreacted versus singly reacted monomers is similar to the ratio for propagation events within the $1.0\sigma_{\text{LJ}}$ shell.

Two other significant results are apparent in Figure 6c. First, the fraction of doubly reacted monomers decreases by ca. 20% when simulating a 50% monovinyl monomer formulation. Alternatively, by simulating polymerization of a comonomer formulation containing 50% monovinyl monomers, the fraction of reacted *divinyl* monomers that are doubly reacted increases by ca. 1.5 (i.e., relative to the divinyl homopolymerization). Second, the fraction of divinyl loops (i.e., solid diamonds) is

approximately the same for both simulated formulations, so the fraction of intramolecular cross-links (i.e., solid squares) decreases by ca. 40% in the formulation containing 50% monovinyl monomers. This observation is reasonable: decreasing the concentration of pendant functionality by 50% causes a proportional decrease in the concentration of intramolecular cross-links.

Model Validation by Experimental Observations. Simulations of the formation of ICMs from individual radicals provide insight into the influences of various reaction parameters on the structure and properties of the polymer that forms at very low overall conversion. Perhaps more importantly, the off-lattice kinetic gelation simulation provides a means to investigate the *evolution* of structure from individual propagation events to interaction of macromolecular species within an evolving network. However, application of the simulation results to characterize only ICMs formed prior to macroscopic gelation has a distinct advantage—experimental validation of the simulated results is feasible. Table 1 contains a summary of selected experimental results that describe the size and structure of ICMs formed from methacrylic anhydride.⁶¹

The apparent agreement between experiments and the simulation results for intramolecular cross-link density is particularly important since the reaction of pendant groups to form doubly reacted monomers is highly dependent on local concentrations of pendant and monomeric moieties (and independent of intramolecular conversion, which will be discussed in the following section). Conversely, the kinetic chain length and ICM size are highly dependent on the somewhat arbitrary designation of a radical's reaction volume, which has a large impact on the probability for a trapping event to occur. Nonetheless, reasonable agreement between simulated ICM characteristics and experimental measurements suggests that the off-lattice kinetic gelation approach is well-suited for investigation of structural evolution at very low conversion.

Conversion-Dependent Evolution of ICM Structure. In the previous sections, final properties of ICMs were characterized after trapping of the propagating radical. In all cases, trapping occurred before the ICM grew larger than the dimensions of the simulation. Since the simulations do not reach the critical conversion (i.e., the macroscopic gel point), comparisons cannot be made to critical exponents known for percolation theory applied to kinetic gelation simulations. Alternatively, the simulated ICMs can be compared to published characteristics of lattice animals, which are the structures formed prior to the critical conversion in percolation simulations.

The fractal dimension of the lattice animal, D_a , is a single parameter that reflects the structure of clusters in percolation models at conversions well below the critical threshold (i.e., the macroscopic gel point). Therefore, values of D_a , relative to conversion and monomer structure, were determined for sets of individual ICMs formed in the off-lattice kinetic gelation simulation. Figure 7 contains double logarithmic plots of the cumulative number of reacted monomers (i.e., combined singly

TABLE 1: Summary of Experimental Characterization of ICMs

ICM characteristic	experimentally determined value ^a	comment on agreement with simulated results
fraction of monomers that are doubly reacted	ca. 30%	good agreement for 120° and 180° monomer simulations
kinetic chain length	ca. 2500 to 5000 repeat units	simulated ICMs are smaller but the largest simulated structures are within a factor of 2
no. of monomers	ca. 1000 to 3000 monomers	simulated ICMs are smaller but the largest simulated structures are within a factor of 2

^a Experimental data from ref 61.

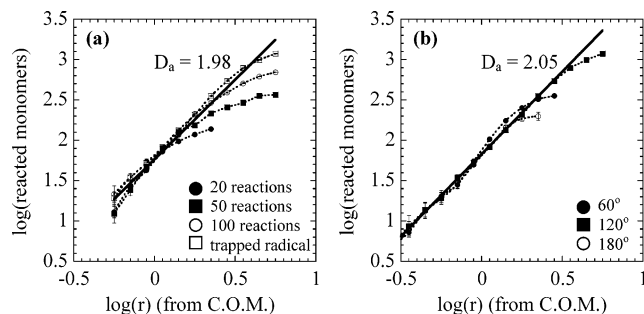


Figure 7. Calculation of fractal dimensions. Double logarithmic plots of the cumulative numbers of reacted monomers as a function of radii from the ICM centers-of-mass are shown. The slope of the linear region in each set of lines corresponds to the fractal dimension (D_a) of the ICM. The numbers of reacted monomers (within radial shells that were ca. $0.5\sigma_{LD}$ thick) were measured, and D_a was calculated at (a) different conversions (i.e., after 20, 50, and 100 reaction attempts) and (b) different divinyl angles within simulation volumes containing 97 336 monomers (divinyl angle in part a, 120° ; monomer mobility, middle level from Figure 4; reaction volume radius, $1.0\sigma_{LD}$).

and doubly reacted) within a radial distance from the center of mass of an ICM. The slope of the line from this analysis is a measure of the fractal dimension of the ICM populations. In Figure 7a, four individual curves correspond to structural data at different degrees of polymerization, averaged for five independent ICMs formed from 120° divinyl monomers. Filled circles correspond to the structural information after 200 attempted propagation steps; filled squares, 500 steps; open circles, 1000 steps; and the open squares correspond to the structural information acquired from five ICMs after trapping of the single propagating radical. All curves have a common slope at short radii, which was measured to be 1.98. This value agrees very well with the theoretical value of 2 for a three-dimensional lattice animal formed prior to the critical conversion.^{62,63} Figure 7b contains an analogous measurement of the fractal dimension for ICMs formed from monomers with different divinyl angles (filled circles, 60° ; filled squares, 120° ; open circles, 180°). Figure 7a,b reveals that the fractal dimension is independent of the degree of polymerization within an ICM or the angle between vinyl groups, and the fractal dimension for both plots is in close agreement with the theoretical value of 2. This value suggests that monomers are incorporated in a random fashion: no preferential propagation direction is observed (which would result in a lower D_a), or alternatively, not all of the monomers within the region containing polymer are incorporated into the network (which would result in a higher D_a).

The same analysis that is depicted in Figure 7 for all singly or doubly reacted monomers was applied to only the doubly reacted monomers. The value of the lattice animal fractal dimension for the doubly reacted monomers, $D_{a,DR}$, was approximately 2.5. This value, which describes the distribution of doubly reacted monomers and reflects the cross-linking structure of the ICM, suggests that the relative concentration of doubly reacted monomers increases at greater distances from the ICM center of mass. In other words, the ICM does not have a more highly cross-linked core surrounded by a shell with a lower density of doubly reacted monomers.

Conclusions

This contribution has reintroduced and added refinements to an off-lattice kinetic gelation model for simulation of multifunctional monomer polymerizations. In particular, more complex monomer structure has been implemented by varying the

angle between reactive vinyl groups on Lennard-Jones spheres that represent monomer units. Furthermore, effects of monomer mobility, structure, and functionality on characteristics of intramolecularly cross-linked macromolecules (ICMs) were reported. Specifically, the relative size, kinetic chain length, and intramolecular cross-link density were explored for ICMs formed from simulation of a single propagating radical within a volume containing ca. 100 000 monomers. Characteristics of simulated ICMs agreed relatively well with analogous experimental information. In addition to exploring specific characteristics of ICMs formed from independent propagating radicals, the fractal dimension of the ICMs formed in this unique simulation were determined. In fact, the lattice animal fractal dimension, which provides information about the internal structure of ICMs, was constant with conversion and monomer structure and matched the theoretical value for three-dimensional percolation.

Acknowledgment. The authors are grateful to Prof. Chris Bowman for discussions regarding the critical behavior of kinetic gelation models. The authors gratefully acknowledge funding for this contribution from the I/UCRC for Fundamentals and Applications of Photopolymerizations, as well as fellowships for J.B.H. from NSF and the Department of Education GAANN programs.

References and Notes

- Hutchison, J. B.; Anseth, K. S. *Macromol. Theory Simul.* **2001**, *10*, 600–607.
- Kloosterboer, J. G. *Adv. Polym. Sci.* **1988**, *84*, 1–61.
- Reisch, M. *Chem. Eng. News* **2001**, *79*, 23–30.
- Dubay, K. *Newspapers Technol.* **2002**, 2003.
- Cook, W. D. *J. Appl. Polym. Sci.* **1991**, *42*, 2209–2222.
- Peppas, N. A.; Huang, Y.; Torres-Lugo, M.; Ward, J. H.; Zhang, J. *Annu. Rev. Biomed. Eng.* **2000**, *2*, 9–29.
- Hubbell, J. A. *Bio-Technology* **1995**, *13*, 565–576.
- Bryant, S. J.; Anseth, K. S. *Biomaterials* **2001**, *22*, 619–626.
- Nguyen, K. T.; West, J. L. *Biomaterials* **2002**, *23*, 4307–4314.
- Whitesides, G. M.; Stroock, A. D. *Phys. Today* **2001**, *54*, 42–48.
- Becker, H.; Locascio, L. E. *Talanta* **2002**, *56*, 267–287.
- Beebe, D. J.; Moore, J. S.; Yu, Q.; Liu, R. H.; Kraft, M. L.; Jo, B. H.; Devadoss, C. *Proc. Natl. Acad. Sci. U.S.A.* **2000**, *97*, 13488–13493.
- Beebe, D. J.; Moore, J. S.; Bauer, J. M.; Yu, Q.; Liu, R. H.; Devadoss, C.; Jo, B. H. *Nature* **2000**, *404*, 588–590.
- Malinsky, J.; Klaban, J.; Dusek, K. *J. Macromol. Sci.—Chem.* **1971**, *A5*, 1071–1085.
- Dusek, K. *Rubber Chem. Technol.* **1982**, *55*, 1–22.
- Berlin, A. A.; Matvejeva, N. G. *Macromol. Rev. Part D—J. Polym. Sci.* **1980**, *15*, 107–206.
- Korolev, G. V.; Bubnova, M. L. *E-Polym.* **2002**, *30*, 1–28.
- Dusek, K.; Duskov-Smrckova, M. *Prog. Polym. Sci.* **2000**, *25*, 1215–1260.
- Nijenhuis, K.; Mijs, W. J., Eds. *Chemical and Physical Networks: Formation and Control of Properties*; John Wiley and Sons: Chichester, UK, 1998; Vol. 1.
- Wen, M.; McCormick, A. V. *Macromolecules* **2000**, *33*, 9247–9254.
- Anseth, K. S.; Anderson, K. J.; Bowman, C. N. *Macromol. Chem. Phys.* **1996**, *197*, 833–848.
- Kinney, A. B.; Scranton, A. B. In *Superabsorbent Polymers*; American Chemical Society: Washington, DC, 1994; Vol. 573, pp 2–26.
- Dusek, K. *Polym. Gels Networks* **1996**, *4*, 383–404.
- Manneville, P.; de Seze, L. In *Numerical Methods in the Study of Critical Phenomena*; Della Dora, J., Demongeot, J., Lacolle, B., Eds.; Springer: Berlin, Germany, 1981; pp 116–124.
- Herrmann, H. J.; Stauffer, D.; Landau, D. P. *J. Phys. A—Math. Gen.* **1983**, *16*, 1221–1239.
- Chhabra, A.; Matthewsorgan, D.; Landau, D. P.; Herrmann, H. J. *J. Phys. A—Math. Gen.* **1985**, *18*, L575–L578.
- Chhabra, A.; Matthewsorgan, D.; Landau, D. P.; Herrmann, H. J. *Phys. Rev. B* **1986**, *34*, 4796–4806.
- Schulz, M. *Prog. Colloid Polym. Sci.* **1992**, *90*, 52–56.
- Lee, S. B.; Jeon, H. J. *Phys. Rev. E* **1997**, *56*, 3274–3280.
- Coniglio, A.; Stanley, H. E.; Klein, W. *Phys. Rev. Lett.* **1979**, *42*, 518–522.

- (31) Coniglio, A.; Stanley, H. E.; Klein, W. *Phys. Rev. B* **1982**, *25*, 6805–6821.
- (32) Bansil, R.; Herrmann, H. J.; Stauffer, D. *Macromolecules* **1984**, *17*, 998–1004.
- (33) Matthewsmorgan, D.; Landau, D. P.; Herrmann, H. J. *Phys. Rev. B* **1984**, *29*, 6328–6334.
- (34) Ghiass, M.; Rey, A. D.; Dabir, B. *Macromol. Theory Simul.* **2001**, *10*, 657–667.
- (35) Liu, Y.; Pandey, R. B. *J. Phys. II* **1994**, *4*, 865–872.
- (36) Bowman, C. N.; Peppas, N. A. *Chem. Eng. Sci.* **1992**, *47*, 1411–1419.
- (37) Bowman, C. N.; Peppas, N. A. *J. Polym. Sci. Part A–Polym. Chem.* **1991**, *29*, 1575–1583.
- (38) Ward, J. H.; Peppas, N. A. *Macromolecules* **2000**, *33*, 5137–5142.
- (39) Wen, M.; Scriven, L. E.; McCormick, A. V. *Macromolecules* **2003**, *36*, 4140–4150.
- (40) Allen, P. E. M.; Bennett, D. J.; Hagias, S.; Hounslow, A. M.; Ross, G. S.; Simon, G. P.; Williams, D. R. G.; Williams, E. H. *Eur. Polym. J.* **1989**, *25*, 785–789.
- (41) Anseth, K. S.; Bowman, C. N. *Chem. Eng. Sci.* **1994**, *49*, 2207–2217.
- (42) Anseth, K. S.; Bowman, C. N. *J. Polym. Sci. Part B–Polym. Phys.* **1995**, *33*, 1769–1780.
- (43) Kloosterboer, J. G.; van de Hei, G. M. M.; Boots, H. M. J. *Polym. Commun.* **1984**, *25*, 354–357.
- (44) Simon, G. P.; Allen, P. E. M.; Bennett, D. J.; Williams, D. R. G.; Williams, E. H. *Macromolecules* **1989**, *22*, 3555–3561.
- (45) Wen, M.; Scriven, L. E.; McCormick, A. V. *Macromolecules* **2003**, *36*, 4151–4159.
- (46) Ghiass, M.; Rey, A. D.; Dabir, B. *Polymer* **2002**, *43*, 989–995.
- (47) Liu, Y.; Pandey, R. B. *Phys. Rev. B* **1997**, *55*, 8257–8266.
- (48) Ward, J. H.; Furman, K.; Peppas, N. A. *J. Appl. Polym. Sci.* **2003**, *89*, 3506–3519.
- (49) Chiu, Y. Y.; Lee, L. J. *J. Polym. Sci. Part A–Polym. Chem.* **1995**, *33*, 269–283.
- (50) Sun, X. D.; Chiu, Y. Y.; Lee, L. J. *Ind. Eng. Chem. Res.* **1997**, *36*, 1343–1351.
- (51) Romantsova, I. I. *Internatl. J. Polym. Mater.* **1993**, *19*, 51–61.
- (52) Hendrickson, R.; Gupta, A.; Macosko, C. W. *Comput. Polym. Sci.* **1995**, *5*, 135–142.
- (53) Leung, Y. K.; Eichinger, B. E. *J. Chem. Phys.* **1984**, *80*, 3877–3884.
- (54) Leung, Y. K.; Eichinger, B. E. *J. Chem. Phys.* **1984**, *80*, 3885–3891.
- (55) Gupta, A. M.; Hendrickson, R. C.; Macosko, C. W. *J. Chem. Phys.* **1991**, *95*, 2097–2108.
- (56) Doherty, D. C.; Holmes, B. N.; Leung, P.; Ross, R. B. *Comput. Theor. Polym. Sci.* **1998**, *8*, 169–178.
- (57) Kurdikar, D. L.; Boots, H. M. J.; Peppas, N. A. *Macromolecules* **1995**, *28*, 5632–5637.
- (58) Boots, H. M. J.; Anseth, K. S.; Kurdikar, D. L.; Peppas, N. A. In *The Wiley Polymer Networks Group Review Series*; te Nijenhuis, K., Mijs, W. J., Eds.; John Wiley and Sons Ltd.: New York, 1998; Vol. 1, pp 377–385.
- (59) Allen, M. P.; Tildesley, D. L. *Computer Simulation of Liquids*; Clarendon Press: Oxford, UK, 1987.
- (60) Noggle, J. H. *Physical Chemistry*, 2nd ed.; Harper Collins Publishers: New York, 1989.
- (61) Hutchison, J. B.; Lindquist, A. S.; Anseth, K. S. *Macromolecules* **2004**, *37*, 3823–3831.
- (62) Stauffer, D.; Aharony, A. *Introduction to Percolation Theory*, 2nd ed.; Taylor and Francis: London, UK, 1992.
- (63) Sahimi, M. *Applications of Percolation Theory*; Taylor and Francis Ltd.: London, UK, 1994.